



## Peptide-grafted dextran vector for efficient and high-loading gene delivery

Journal:	<i>Biomaterials Science</i>
Manuscript ID	BM-ART-10-2018-001341.R1
Article Type:	Paper
Date Submitted by the Author:	20-Nov-2018
Complete List of Authors:	Hu, Yang; Beijing University of Chemical Technology, Biomaterials Wang, Huifeng; University of Illinois at Chicago, Chemical Engineering Song, Haiqing; University of Illinois at Chicago, Chemical Engineering Young, Megan; University of Illinois at Chicago, Chemical Engineering Fan, Yaqian; Beijing University of Chemical Technology, Biomaterials Xu, Fujian; Beijing University of Chemical Technology, Biomaterials Qu, Xinjian; University of Illinois at Chicago Lei, Xia; University of Akron, Department of Chemical and Biomolecular Engineering Liu, Ying; University of Illinois, Chemical Engineering Cheng, Gang; University of Illinois at Chicago, Chemical Engineering

**Peptide-grafted dextran vector for efficient and high-loading gene delivery**

Yang Hu,<sup>1,2</sup> Huifeng Wang,<sup>2</sup> Haiqing Song,<sup>2</sup> Megan Young,<sup>2</sup> Yaqian Fan,<sup>1</sup> Fu-Jian Xu,<sup>1</sup>  
Xinjian Qu<sup>2</sup>, Xia Lei,<sup>3</sup> Ying Liu,<sup>2</sup> Gang Cheng<sup>2,3,\*</sup>

<sup>1</sup>State Key Laboratory of Chemical Resource Engineering, Beijing Laboratory of Biomedical Materials, Beijing University of Chemical Technology, Beijing 100029, China

<sup>2</sup>Department of Chemical Engineering, University of Illinois at Chicago, Chicago, IL 60607, United States

<sup>3</sup>Department of Chemical and Biomolecular Engineering, University of Akron, Akron, OH 44325, United States

\* To whom correspondence should be addressed

E-mail addresses: gancheng@uic.edu

**Abstract**

Among various polymeric gene delivery systems, peptide-based vectors demonstrate great potential owing to their unique structure and property flexibility; however, the molecular understanding on the role and properties of amino acid building blocks in gene delivery is insufficient. In this work, we constructed a series of histidine (H)-contained peptide-grafted dextran (D-RxHy) vectors via a simple two-step reaction of dextran with five RxHyC peptides: R7H3C, R5H3C, R5H5C, R3H5C, and R3H7C. The gel electrophoresis study unveiled the DNA-binding ability of H residues. While all D-RxHy vectors possess similarly low cytotoxicity, D-R3H7 exhibited the highest gene transfection efficiency. Interestingly, at the low nitrogen to phosphate (N/P) ratio of 2, D-R3H7 displayed a 6–8-fold higher luciferase expression compared to the gold standard branched PEI (25k). D-R3H7 and D-R5H5 demonstrated favorable cell uptake rates. A chloroquine-treated transfection assay confirmed the key effect of the high buffering capacity of H-rich D-R3H7 on its high gene transfection efficiency, especially at low N/P ratios. The present work unveiled that histidine is critical for both DNA condensation and the accurate control of endosomal escape. The tunable D-RxHy platform not only demonstrates a promising potential for therapeutic purposes but can also be used as a tool to elucidate the molecular mechanism of the polymer-based transfection.

**Keywords:** Gene delivery; high-loading vector; peptide; histidine; dextran.

## 1. Introduction

Gene therapy has been recognized for decades as a promising strategy for the many challenging diseases, such as cancers and genetic diseases [1-3]. The recent advances in molecular biology, such as genome editing techniques [4,5], have led to the rapid development of gene therapy where highly efficient and safe gene vectors are crucial. A critical cause that rendered gene delivery challenging is the requirement of vectors with accurately balanced properties. In comparison with viral vectors, a series of liposome and polymeric vectors have been developed owing to the low host immunogenicity and low-cost large-scale production [6-8]. Although significant efforts have been devoted to developing polymer-based DNA delivery systems, no polymer-based delivery system has progressed to clinical trials thus far as the properties of the current polymer-based vectors can only be adjusted discontinuously, thus leading to unsatisfactory results and omission of molecular details. Recently, natural materials, such as cationic polysaccharides [9-11] and (poly)peptides [12-14], have been particularly appealing for the design of new polymeric vectors because of their high biocompatibility and degradability.

Among the natural materials, cationic chitosan and its derivatives have been utilized intensively for gene vectors [10,11]. However, the unsatisfactory gene transfection ability limits their effective applications. A series of cationized polysaccharides has been constructed via the introduction of cationic molecules or polymers onto nonionic polysaccharides [15-17]. These cationized polysaccharides with tunable structure could achieve good gene transfection performance including high transfection efficiency and moderate toxicity. Nevertheless, the gene transfection efficiency relies on the high ratio of the cationic polymer's amine to the DNA phosphate group (N/P ratio) [16,17]. These

studies indicated that the drug loading efficiency of such polysaccharide-based vectors was in general low, thus restricting their applications for *in vivo* gene delivery, as the higher ratio of positively charged vector materials leads to toxicity concerns. Although polysaccharides alone as the vectors exhibit some drawbacks owing to the lack of the desired functional groups, they can serve as molecular binders perfectly.

Peptides are another group of natural materials that have been studied extensively for gene delivery because one major advantage of the peptide-based materials is that their properties can be finely tuned in a nearly continuous manner. Buschmann *et al.* revealed that a high N/P ratio, or excess cationic polymer, enhanced the gene transfection efficiency by promoting endosome escape [18]. Histidine (H), owing to its high buffering capacity, has been introduced onto polymeric gene vectors to benefit endosome escape and improve transfection efficiency [19-21]. However, large peptides (> 15aa) are expensive. To utilize peptide and reduce the cost, our group has constructed a dextran-peptide vector consisting of a dextran backbone and an H-containing cationic peptide [22]. Nevertheless, such H-containing dextran-peptide platform can be further optimized for better gene delivery, such as high-loading delivery, via rational design on different constituents of peptides. Based on previous studies, we hypothesize that histidine is critical in peptide-based gene delivery vector design. Thus far, to our best knowledge, research work on the gene transfection behaviors of concisely tailored introduction of H have not been reported yet. To understand the role of H in peptide-based gene delivery vector at the molecular level, we designed five RxHyC cationic peptides (R7H3C, R5H3C, R5H5C, R3H5C, and R3H7C), composed of one C-terminal cysteine residue and varied numbers of arginine (R) and H residues. RxHyC cationic peptides were

grafted to dextran to construct a series of comb-shaped dextran-peptide (D-RxHy) vectors. The performance of such D-RxHy vectors in gene delivery was investigated in terms of DNA-binding capability, cytotoxicity, gene transfection, cell internalization, and endosome escape.

## 2. Materials and methods

### 2.1. Materials

Dextran (15–25 kDa), glycidyl methacrylate (GMA), dimethyl sulfoxide, branched polyethylenimine (PEI, 25 kDa), and chloroquine (CQ) were purchased from Sigma–Aldrich (St. Louis, MO). 4-(dimethylamino) pyridine (DMAP) and tris(2-carboxyethyl)phosphine hydrochloride (TCEP) were purchased from Chem-Impex International (Wood Dale, IL). Five RxHyC peptides NH<sub>2</sub>-RRRRRRRHHHC-COOH (R7H3C), NH<sub>2</sub>-RRRRRHHHC-COOH (R5H3C), NH<sub>2</sub>-RRRRRHHHHHC-COOH (R5H5C), NH<sub>2</sub>-RRRHHHHHC-COOH (R3H5C), NH<sub>2</sub>-RRRHHHHHHHC-COOH (R3H7C)—were designed by our lab and synthesized by Genscript (Piscataway, NJ). Agarose, trypsin-acetate-EDTA (TAE) buffer, and 3-(4,5-dimethylthiazol-2-yl)-2,5-diphenyltetrazolium bromide (MTT) were purchased from Alfa Aesar (Haverhill, MA). Agarose, DNA loading buffer, Dulbecco's modified eagle medium (DMEM), penicillin/streptomycin, fetal bovine serum (FBS), L-Glutamine, nonessential amino acids, and trypsin were purchased from VWR International (Radnor, PA). GelRed™ nucleic acid gel stain and YOYO™-1 Iodide nucleic acid fluorescent dye (YOYO) were purchased from Biotium Inc. (Fremont, CA) and Thermo Fisher Scientific (Waltham, MA), respectively. Plasmid pCMV-luc encoding a firefly luciferase and plasmid pEGFP-N1 encoding an enhanced green fluorescent protein (EGFP) were purchased from Elim

Biopharmaceuticals (Hayward, CA). The COS7 and MCF7 cell lines were purchased from the American Type Culture Collection (Manassas, VA). The cell lines were cultured at 37 °C under a 5% CO<sub>2</sub> atmosphere in a typical culture medium—DMEM medium supplemented with nonessential amino acids, L-Glutamine, penicillin–streptomycin, and 10% FBS.

## *2.2. Synthesis of RxHyC peptide-grafted dextran (D-RxHy) vector*

As shown in Figure 1, a simple two-step method was adopted to prepare RxHyC peptide-grafted dextran (D-RxHy) vectors. First, methacrylate (MA)-functionalized dextran (Dex-MA) was synthesized by the transesterification reaction of the hydroxyl groups of dextran with GMA using DMAP as a catalyst [22,23]. The procedures are based on our previous paper [22], with a feed of dextran (1.0 g, containing 6.2 mmol glucose units), GMA (330 μL, 2.5 mmol), and DMAP (1.0 g). After four days of reaction, the mixture was neutralized with concentrated HCl at an equimolar amount of DMAP. Subsequently, the reaction mixture was dialyzed for four days against deionized (DI) water in the dark, and then freeze-dried and analyzed with <sup>1</sup>H NMR.

Next, RxHyC peptides with a terminal cysteine residue were conjugated with the MA groups of Dex-MA via the highly efficient Michael-type reaction [22]. Using R7H3C as an example, the procedures are as follows: R7H3C (40 mg, 0.025 mmol) was dissolved with 100 μL of DI water, subsequently added with 25 μL of TCEP (200 mM), and incubated for 5 min at room temperature. Subsequently, the acidic mixture, owing to the TCEP and trifluoroacetic acid from peptide synthesis, was neutralized by NaOH (1M). Dex-MA (11 mg, containing 0.021 mmol MA groups) was dissolved in 50 μL of DI

water in a separate tube and sonicated for 5 min. The R3H7C solution was added to the Dex-MA solution and the mixture was added with NaOH (1M) for a final pH of 7.5. The mixture was reacted for two days at room temperature under a gentle shake. The produced D-R7H3 was purified with a Zeba spin (MWCO 7000) desalting column (Thermo Fisher Scientific, Waltham, MA), and then freeze-dried and analyzed with  $^1\text{H}$  NMR.

### *2.3. Preparation and characterization of D-RxHy/pDNA polyplexes*

The plasmid DNA (pDNA) solution was prepared by diluting plasmid pCMV-luc to the concentration of 0.1 mg/mL in nuclease-free water. All D-RxHy vectors were dissolved at the nitrogen (N) concentration of 10 mM in nuclease-free water to prepare the stock solutions. Here, the N content was determined by the number of arginine residues in each D-RxHy vector. Each mixture of D-RxHy and pDNA was vortexed and incubated for 0.5 h to form the polymer/pDNA complex (polyplex) at the pre-determined N/P ratio. The N/P ratio was defined as the molar ratio of N in D-RxHy vector to phosphate (P) in pDNA. The DNA-binding ability of the D-RxHy vector was evaluated by the agarose gel electrophoresis assay of D-RxHy/pDNA polyplexes, using typical procedures [24]. The particle size and zeta potential of D-RxHy/pDNA polyplexes were assessed with a Zetasizer system (Malvern NanoZS, UK) [24].

### *2.4. Cytotoxicity assay*

The cytotoxicity of D-RxHy/pDNA polyplexes was evaluated in COS7 and MCF7 cell lines. The cells were seeded in a 96-well plate ( $10^4$ /well) and incubated in 100  $\mu\text{L}$  of

typical medium for 24 h. Subsequently, the old medium in each well was replaced with 100  $\mu\text{L}$  of fresh medium containing D-RxHy/pDNA polyplexes (0.33  $\mu\text{g}$  pDNA) at various N/P ratios, and the cells were incubated for 4 h. Next, the medium containing D-RxHy/pDNA polyplexes was replaced by 100  $\mu\text{L}$  of fresh medium, and the cells were incubated for another 20 h to achieve the total transfection time of 24 h. Finally, the viability of cells in each well were measured by an MTT assay, according to the procedures in our previous paper [22]. The untreated cells were used as the control group and the relative cell viabilities of D-RxHy/pDNA polyplexes at various N/P ratios were expressed as a percentage of the control group. Six replicates were performed in the cytotoxicity assay.

### 2.5. *In vitro* gene transfection assay

The *in vitro* transfection assay of D-RxHy/pDNA polyplexes was first performed in COS7 and MCF7 cell lines, using pCMV-luc encoding a firefly luciferase as the reporter gene. The cells were seeded in a 24-well plate ( $5 \times 10^4$ /well) and incubated in 500  $\mu\text{L}$  of typical medium for 24 h. Subsequently, the old medium in each well was replaced with 500  $\mu\text{L}$  of fresh medium containing D-RxHy/pDNA polyplexes (1.0  $\mu\text{g}$  pDNA) at various N/P ratios, and the cells were incubated for 4 h. Next, the medium containing D-RxHy/pDNA polyplexes was replaced by 500  $\mu\text{L}$  of fresh medium, and the cells were incubated for another 20 h. After incubation, the old medium was removed, the cells were washed with PBS twice, and each well was added with 200  $\mu\text{L}$  of Promega lysis buffer (Madison, WI) to lyse the cells. Finally, the luciferase expression and protein content of the cells in each well were measured by the Promega luciferase assay kit (Madison, WI),

and the Thermo Scientific BCA protein assay kit (Waltham, MA), respectively. The luciferase expression efficiencies of D-RxHy/pDNA polyplexes (RLU/mg protein) were expressed as relative light unit (RLU) per milligram of protein lysate. Three replicates were performed in the luciferase expression assay.

The *in vitro* luciferase transfection assay of D-RxHy/pDNA polyplexes treated with CQ was also performed in the MCF7 cell line, according to a previous paper [18]. The transfection procedures were as described above, except that the cell was incubated with 500  $\mu$ L of fresh medium containing D-RxHy/pDNA polyplexes (1.0  $\mu$ g pDNA) at various N/P ratios and 75  $\mu$ M concentration of CQ for 4 h. Thereafter, the medium was replaced with 500  $\mu$ L of fresh CQ-free medium, and the cells were incubated for another 20 h.

A gene transfection assay was also performed in MCF7 cells using plasmid pEGFP-N1 encoding EGFP as the reporter gene. The same transfection procedures as for luciferase expression were adopted. After 24 h of transfection, the MCF7 cells were imaged using an Olympus IX81 fluorescence microscope (Olympus, Japan). The percentage of EGFP-transfected (positive) cells was determined using Beckman cyan flow cytometry (Beckman Coulter, USA) [24].

### *2.6. Cellular internalization assay*

The cellular internalization assay of D-RxHy/pDNA polyplexes was first performed in the MCF7 cell line, using fluorescent pCMV-luc labeled with Thermo Scientific YOYO-1 dye (Waltham, MA) [24]. D-RxHy/labeled pRL-CMV polyplexes were prepared as described above. MCF7 cells were seeded in a six-well plate ( $6 \times 10^5$ /well) and incubated in 2 mL of typical medium for 24 h. Subsequently, the old medium in each well was

replaced with 2 mL of fresh medium containing D-RxHy/pDNA polyplexes (6.0  $\mu$ g pDNA) at various N/P ratios. The cells were incubated for 4 h; subsequently, the medium containing D-RxHy/pDNA polyplexes was removed. Finally, the cells were washed with PBS twice, digested by trypsin, and assessed by Beckman cyan flow cytometry (Beckman Coulter, USA).

### *2.7. Buffering capacity assay*

The buffering capacity of D-RxHy vectors in the pH range of 4–7 was determined by acid–base titration, according to similar procedures in our previous paper [16]. Further, 5 mL of D-RxHy solutions at an arginine concentration of 1 mM were prepared in DI water, and the pH of the solutions was adjusted to pH 7 using HCl or NaOH. Subsequently, the D-RxHy solutions were titrated against 0.01 N HCl solution by adding 50  $\mu$ L of HCl solution each time until the pH reached 4. The change in pH was measured by a pH meter. The PEI solution at an amino concentration of 1 mM was prepared and titrated as the control group.

### *2.8. Statistical analysis*

All experiments were repeated at least three times. Data were presented as means  $\pm$  standard deviation. Statistical significance was evaluated by Student's t-test when two groups were compared. If more than two groups were compared, statistical significance was evaluated using one-way analysis of variance (ANOVA) followed by Bonferroni's post hoc test.

### 3. Results and discussion

#### 3.1. Synthesis and characterization of D-RxHy vectors

To prepare the comb-shaped D-RxHy vectors via the thiol-based “graft to” method, it is essential to introduce electron-poor alkene onto dextran (Figure 1). In this work, a fraction of the hydroxyl groups in dextran were functionalized with methacryloyl (MA) groups via the transesterification reaction of GMA and dextran [22,23], producing Dex-MA. The  $^1\text{H}$  NMR spectrum of Dex-MA is shown and analyzed in detail in the Supporting Information (Figure S1). Based on the  $^1\text{H}$  NMR data, approximately one-third glucose units of dextran were functionalized with the MA group. There are two advantages of using this chemistry. First, the degree of the substitution (DS) of MA can be well controlled by adjusting the feed ratio of GMA to dextran. Next, the ester bond between MA and dextran can be hydrolyzed to produce dextran at the original state with minimal chronic toxicity. Five RxHyC peptides (R7H3C, R5H3C, R5H5C, R3H5C, and R3H7C), composed of one C-terminal cysteine residue and varying numbers of arginine (R) and histidine (H) residues, were grafted to Dex-MA via the highly efficient thiol-(meth)acrylate Michael addition reaction [22]. The produced D-RxHy vectors were termed as D-RxHy, based on the sequence of the grafted RxHyC peptide. The  $^1\text{H}$  NMR spectra of D-RxHy hybrids are shown and analyzed in detail in the Supporting Information (Figure S1). Based on the  $^1\text{H}$  NMR data, the average DS of the peptide side chains for D-R7H3, D-R5H3, D-R5H5, D-R3H5, and D-R3H7 were 15.5%, 16.2%, 16.6%, 15.7%, and 17.4%, respectively. Five D-RxHy hybrids possessed approximately the same grafting ratio of peptide side chains. To be noted, such grafting ratios of RxHyC peptides in five D-RxHy hybrid materials were much less than the DS of MA (~35%) in

Dex-MA. Because the conjugation of Dex-MA and RxHy peptide was reacted at the pH of 7.5 for 2 days, the hydrolysis of ester linkages between MA group and dextran leads to in the low grafting ratio (15~17%).

### *3.2. Biophysical characterization of D-RxHy/pDNA polyplexes*

For a successful nucleic acid delivery, the vectors are required to bind and condense pDNA into nanostructured polymer/pDNA complexes (polyplexes), which can protect pDNA from degradation and facilitate cellular uptake. The polymeric gene delivery vector can interact with pDNA via either electrostatic interaction [16] or hydrogen bond [25]. The binding affinity between the vector and nucleic acids determines the size/surface charge of the polyplexes, stability of polyplex in the blood, and release of payload in the cell. In this work, the DNA-binding affinity of D-RxHy vectors was first evaluated by agarose gel electrophoresis (Figure 2). Compared to the naked pDNA, the mobility of pDNA decreased with increasing N/P ratio for all D-RxHys, indicating the formation of D-RxHy/pDNA polyplexes. For different D-RxHy vectors, the complete retardation of pDNA was observed at different threshold N/P ratios. As shown in Figure 2a, 2b', 2c, and 2d, the threshold N/P ratios of D-R5H3 and D-R3H5 were 6 and 2.5, which were higher than that of D-R7H3 and D-R5H5 (5 and 2, respectively). With the same number of H residues, the increased amount of R residues in RxHyC peptides enhanced the DNA-binding ability of D-RxHy vectors. It was well-known that the DNA-binding ability of polymer vectors increases with the molecular weight of cationic chains [26]. Interestingly, the threshold N/P ratios of D-R7H3, D-R5H5, and D-R3H7 are 5, 2, and 1, respectively. This indicates that the order of DNA-binding ability is D-R7H3<D-

R5H5<D-R3H7 even though D-R7H3 has a higher R ratio. The N/P ratio is calculated as the molar ratio of the guanidine group of arginine to phosphate group of pDNA, as only a small portion of H residues are protonated at pH >6. Considering the same number (10) of R+H residues, it can be inferred that the increased amount of H residues increases the DNA-binding ability of RxHyC peptides. The agarose gel electrophoresis results indicated that both R and H residues of RxHyC peptides contributed to the DNA-binding ability of D-RxHy vectors.

The structure of vector/DNA polyplexes is important to modulate their cellular uptake [24]. The particle size and zeta potential of D-RxHy/pDNA polyplexes at the N/P ratio from 2 to 20 were determined by dynamic light scattering (DLS), and the results are shown in Figure 3. At a low N/P ratio of 2, both D-R7H3 and D-R3H5 condensed the DNA into obviously larger particles than D-R5H5 and D-R3H7. Meanwhile, the particle size of D-R5H3/pDNA polyplexes was the largest at the N/P ratio of 2 (Figure 3a). Such results can be attributed to the different DNA-binding ability of D-RxHy vectors because at low N/P ratios, polycation vectors with low DNA-binding ability lead to larger polyplexes. At most N/P ratios, D-RxHy/pDNA polyplexes showed decreased particle size with increasing N/P ratio. At higher N/P ratios (> 5), the higher amount of cationic D-RxHy benefits the complexation process with pDNA. Notably, D-R5H5 and D-R3H7 condensed pDNA into the smallest nanoparticles (75–125 nm) at all N/P ratios, even at the low N/P ratio of 2. Such small particle size further confirmed the excellent DNA-binding ability of D-R5H5 and D-R3H7.

The zeta potential indicates the surface charges of the vector/DNA polyplexes. As shown in Figure 3b, at low N/P ratios of 2 and 5, D-R7H3/pDNA polyplexes showed the

highest zeta potential among the D-RxHy/pDNA polyplexes. R7H3C peptide possessed the highest amount of cationic R residues among all tested peptides and resulted in the highest charge density of D-R7H3. Although the gel electrophoresis results demonstrated the DNA-binding ability of H residues (Figure 2), the zeta potential of polyplexes was primarily determined by the cationic density of D-RxHy peptides. At the N/P ratios of 10 and above, the zeta potentials of the polyplexes were not affected by the excessive amount of D-RxHys. Meanwhile, all D-RxHy/pDNA polyplexes exhibited positive zeta potential, indicating their positive surface charges. Such positively charged surfaces, as well as the desirable/small particle size, would benefit the electrostatic interaction with cell membranes and the subsequent cellular uptake.

### *3.3. Cell viability*

The cytotoxicity of D-RxHy/pDNA polyplexes was evaluated by the MTT assay in COS7 and MCF7 cells, using PEI/pDNA polyplexes (N/P = 10) as a control (Figure 4). Generally, all D-RxHy/pDNA polyplexes exhibited low cell toxicity (cell viability > 80%) at the N/P ratio of 2, and followed a slightly dose-dependent toxicity with increasing N/P ratio. Compared to PEI, five D-RxHys condensed pDNA into polyplexes with lower toxicity at the N/P ratios of 10 and below. The lower toxicity of the D-RxHy vectors can be attributed to the nontoxic dextran backbone and short peptide side chains. Other cationic polysaccharide vectors have also been reported with similarly low toxicity [17,26], in which polysaccharides (such as dextran, pullulan) were grafted with short cationic polymer chains. As mentioned above, D-R5H5 and D-R3H7 exhibited much higher DNA-binding ability than the other three D-RxHys. It was reported that the

polymeric vectors of high DNA-binding ability would typically occur with long cationic polymer chains and the resultant high toxicity [17,26]. However, D-R5H5/pDNA and D-R3H7/pDNA polyplexes demonstrated no obvious difference in toxicity with the other D-RxHy/pDNA polyplexes at all the same N/P ratios (Figure 4). This indicates that the incorporation of H residues can yield lower toxicity despite its high DNA-binding ability.

#### 3.4. *In vitro* gene transfection

To study the transfection efficiency of D-RxHy vectors, an *in vitro* luciferase protein expression assay using pCMV-luc plasmid was first evaluated in COS7 and MCF7 cell lines (Figure 5). PEI/pDNA polyplex (N/P = 10) was used as a control [16,24]. With the increase in N/P ratio from 2 to 20, the luciferase expression level of D-RxHy vectors except D-R3H7 increased initially, followed with a decreasing trend. However, at low N/P ratios, D-RxHy vectors except D-R3H7 could not condense pDNA efficiently, especially for D-R7H3 and D-R5H3 at the N/P ratio of 2. At high N/P ratios, the presence of excessive D-RxHy increases cytotoxicity. Such a trend is consistent with that of the reported polymeric gene vectors [16,17]. On the contrary, D-R3H7 mediated the highest luciferase expression at the low N/P ratio of 2, which decreased slightly with increasing N/P ratio. As mentioned above, D-R3H7 possesses the highest DNA-binding ability among five D-RxHy vectors, and could completely condense pDNA into positively charged polyplexes at the low N/P ratio of 1 (Figure 2). Moreover, H residues of RxHy peptide would be protonated, become positively charged in acidic condition in endosome and further enhance the DNA-binding ability of D-RxHy vectors. The strong DNA-binding ability and high ratio of H to R residues of D-R3H7 might jeopardize the

disassembly of D-R3H7/DNA polyplexes in cells at the high N/P ratios, and therefore reduce the transfection efficiency.

Nevertheless, D-R3H7 at the N/P ratio of 2 exhibited the highest luciferase expression level among five D-RxHy vectors, which is 6.5 fold and 8.1 fold compared to PEI/pDNA polyplex in COS7 and MCF7 cell lines, respectively (Figure 10). Combined with the high cell viability of D-R3H7 (89.7% in COS7 and 98.0% in MCF7 cell lines) at the optimal N/P ratio of 2, such results demonstrate the excellent gene transfection performance of D-R3H7.

Interestingly, when the ratio of H to R residues in the corresponding RxHyC peptide increased (Figure 1) from D-R7H3 to D-R3H7, the corresponding luciferase expression level increased accordingly at the low N/P ratio of 2 in both the COS7 and MCF7 cell lines. Such different transfection behaviors imply that the amount of H residues in RxHyC peptides affect the gene transfection ability of D-RxHy vectors significantly. This can be explained by two important factors observed in this study. First, the smaller particle size of D-R5H5/pDNA and D-R3H7/pDNA polyplexes (especially at low N/P ratios of 2 and 5, Figure 3a) would lead to enhanced cellular uptake efficiency. This will be discussed in detail in section 3.5. Next, the introduction of imidazole groups has been reported to enhance the buffering capacity of polymeric vectors [19,21]. Owing to the same DS/grafting ratio and the highest relative amount of H residues in R3H7C peptide, D-R3H7 likely possessed the highest buffering capacity and would lead to the most efficient endosome escape of D-RxHy/pDNA polyplexes. This will be discussed and confirmed in detail in Section 3.6.

With the same amount of H residues in the corresponding RxHyC peptides, the optimal transfection efficiencies of D-R7H3 and D-R5H5 were comparable to that of D-R5H3 and D-R3H5, respectively (Figure 5). Thus, D-R7H3 and D-R5H5 were chosen to compare with D-R3H7 in the following analysis tests in this work. To further understand the excellent gene delivery ability of D-R3H7, the *in vitro* enhanced green fluorescent protein (EGFP) transfection assay using pEGFP-N1 plasmid was also performed in the MCF7 cell line. The direct visualization of D-R7H3-, D-R5H5-, and D-R3H7-mediated EGFP expressions were performed using fluorescence microscopy, where the EGFP expression in cells displayed green fluorescence. As shown in Figure 6a<sub>1</sub>, 6b<sub>1</sub>, and 6c<sub>1</sub>, the MCF7 cells transfected by D-R7H3/pEGFP-N1 exhibited a significantly lower amount of green signal cells than cells transfected by D-R5H5/pEGFP-N1 and D-R3H7/pEGFP-N1 at the low N/P ratio of 2. The percentages of EGFP-positive cells, determined by flow cytometry, were 1.2%, 7.3%, and 19.4% for D-R7H3, D-R5H5, and D-R3H7, respectively. Meanwhile, PEI lead to 6.3% EGFP-positive cells at its optimal N/P ratio of 10 (Figure S2, Supporting Information). The higher EGFP expression of D-R3H7 was consistent with the luciferase expression results (Figure 5), further confirming its excellent transfection ability at the low N/P ratio. With the N/P ratio increased to 10 (Figure 6a<sub>2</sub> and 6b<sub>2</sub>), the percentages of EGFP-positive cells for D-R7H3 and D-R5H5 increased to 9.0% and 12.2%, respectively. On the contrary, D-R3H7 exhibited a 20.4% of EGFP-positive cells at the N/P ratio of 10, almost the same with that at the N/P ratio of 2. This indicated that different D-RxHy demonstrated different EGFP expression behaviors with increasing N/P ratio, and the underlying mechanism will be investigated in the following Sections 3.5 and 3.6. Notably, D-R5H5 vector produces a lower

percentage of EGFP-positive cells (12.2% vs. 20.4%) than D-R3H7 vector, but the luciferase expression level of D-R5H5 was higher than that of D-R3H7 (Figure 5b). Such difference can be attributed to the nature of the assay. Luciferase assay indicated the total luciferase expression level while EGFP assay indicated the percentage of EGFP (protein)-positive cells. The detected luciferase level can be very high even a small fraction of cells expressing luciferase at a very high level. In addition, at the N/P ratio of 10, D-R5H5 mediated a higher mean fluorescence intensity of EGFP-positive cells (1504 vs. 1261) than D-R3H7. Both the luciferase and EGFP expression results confirmed that the gene delivery ability of D-RxHy vectors could be optimized by tuning the structure of RxHyC peptides. D-R3H7, with a higher H ratio in RxHyC side chains, demonstrates promise for the high-efficient delivery of plasmids at low N/P ratios.

### *3.5. Cellular internalization*

A high cellular internalization is a prerequisite for all efficient gene delivery systems [24]. In this study, the cellular uptake rates of D-RxHy/pDNA polyplexes were evaluated in MCF7 cells by flow cytometry, using pCMV-luc plasmid labeled with YOYO. To understand the differences in transfection ability, D-R7H3, D-R5H5, and D-R3H7 were all tested with the polyplexes at the low N/P ratio of 2, and the high N/P ratio of 10. As shown in Figure 7a<sub>1</sub>, 7b<sub>1</sub>, and 7c<sub>1</sub>, D-R5H5/pDNA and D-R3H7/pDNA polyplexes demonstrated significantly higher cell uptake rate (percentage of YOYO-positive cells) than D-R7H3/pDNA polyplexes at the N/P ratio of 2. The lower cell uptake rate of D-R7H3/pDNA polyplexes was caused by its lower DNA-binding ability and larger particle size (Figure 2 and 3), thus leading to the worse transfection performance. Interestingly,

D-R3H7 mediated a much higher luciferase and EGFP expression than D-R5H5, despite the similar cell uptake rate of approximately 95.0% (Figure 5 and 6). This might be caused by the less efficient endosomal escape and/or DNA release of D-R5H5. The DNA-binding ability of D-R5H5 might be sufficiently strong for forming polyplexes of small particle size and realizing the high cellular internalization. The higher ratio of H residues in D-R3H7 might benefit the intracellular pDNA delivery and the resultant transfection efficiency.

When the N/P ratio increasing from 2 to 10 (Figure 7a<sub>2</sub> and 7b<sub>2</sub>), the percentage of YOYO-positive cells for D-R7H3 and D-R5H5 slightly decreases to 80.2% and 80.6%, respectively. However, both D-R7H3 and D-R5H5 showed higher gene transfection at the N/P ratio of 10 than at the N/P ratio of 2. D-R<sub>x</sub>H<sub>y</sub> condensed pDNA into more compacted polyplexes at the high N/P ratio of 10 than the N/P ratio of 2 that would display lower fluorescence intensity. As shown in Figure 8, the mean fluorescence intensities of YOYO-positive cells for D-R7H3 and D-R5H5 were both below 50 at the N/P ratio of 10, which is obviously lower than those at the N/P ratio of 2. At the N/P ratio of 10, some MCF7 cells with a low amount of fluorescent polyplexes could be calculated to be YOYO-negative cells, and therefore exhibited a lower percentage of YOYO-positive cells. Moreover, the transfection efficiency of D-R5H5 is higher than that of D-R7H3 at the N/P ratio of 10, despite the similar cell uptake rate. As mentioned above, the higher amount ratio of H residues in D-R5H5 might benefit the intracellular pDNA delivery. Notably, for D-R3H7, the mean fluorescence intensities of YOYO-positive cells were approximately 250 and below 50 at the N/P ratio of 2 and 10, respectively (Figure 8). It indicated that D-R3H7/pDNA polyplex also became more compacted at higher N/P

ratios, despite its ability to completely condense pDNA into positively charged polyplexes at a low N/P ratio of 1 (Figure 2). Therefore, the reason of the transfection efficiencies of D-R3H7 were not enhanced by increasing the N/P ratio was that the high DNA-binding ability of D-R3H7 could compromise the intracellular disassembly of D-R3H7/DNA polyplexes (of high N/P ratio).

### 3.6. Endosomal escape

The polymer/DNA polyplexes will be transported into the endosome and the subsequent lysosome after entering the cells via endocytosis. As shown in Figure 1, endosomal escape is an important factor for the delivery of DNA and the resultant gene transfection. The buffering capacity of polymeric vectors has a prominent effect on the efficiency of endosome escape [16]. The buffering ability of different D-RxHy vectors was evaluated using acid–base titration under the given 1-mM cationic group (R residue) concentration. As shown in Figure 9, the order of buffering capacity ability is D-R7H3<D-R5H5<D-R3H7. It demonstrated that the buffering capacity of D-RxHy vectors increased significantly with the increasing ratio of H residues in RxHyC peptides. At low N/P ratios, the amount of excessive/free D-RxHy is low in the D-RxHy/pDNA polyplexes. The endosome escape of such polyplexes was determined primarily by the buffering capacity of D-RxHy vectors. This would explain why D-R3H7 exhibited a significantly higher transfection efficiency than D-R5H5 and D-R7H3 at the N/P ratio of 2 (Figure 5 and 6). PEI, as a well-known polymeric vector with high buffering capacity, was used as the control and titrated groups under the 1 mM amino group concentration. PEI indicated a slightly lower buffering capacity than D-R5H5 in the pH range of 7 to 5. As shown in Figure 7, PEI indicated a higher cell uptake rate than D-R5H5 at the N/P

ratio of 10 (95.2% vs. 80.6%), while the latter exhibited a higher luciferase and EGFP expression efficiency. Such difference was attributed to the higher buffering capacity of D-R5H5 and the resultant more efficient endosome escape. It indicated that the buffering capacity was critical in the transfection efficiency of polymeric vectors.

To further demonstrate the effect of buffering capacity difference on gene transfection efficiency, a chloroquine (CQ)-treated luciferase expression assay was evaluated in MCF7 cells for different D-RxHy vectors and PEI control (Figure 10). CQ can function as an endosome-disrupting agent that can enter endosomes with polyplexes, and resist with their acidification process owing to its strong buffering capacity [18]. Incubation with CQ has been proven to increase the transfection efficiency of polycation/pDNA polyplexes if the delivery system lacks buffering capacity [18,27-29]. At its optimal N/P ratio of 10, the transfection efficiency of PEI/pDNA polyplex with CQ was 2.2-fold higher than PEI/pDNA polyplex only. This indicated that the buffering capacity of PEI could be further enhanced to achieve more efficient endosome escape and better transfection. As shown in Figure 10, D-R7H3, D-R5H5, and D-R3H7 showed different transfection behaviors under the treatment of CQ at the low N/P ratio of 2. At the CQ concentration of 75  $\mu\text{M}$ , the transfection efficiencies of D-R7H3 and D-R5H5 were enhanced 7.3-fold and 1.4-fold compared to the absence of CQ treatment, respectively. On the contrary, D-R3H7/pDNA polyplexes demonstrated significantly decreased luciferase expression after the CQ treatment. As mentioned above, the buffering capacity of D-RxHy vectors is crucial on the endosome escape of polyplexes at low N/P ratio. D-R7H3, with the lowest buffering capacity, benefitted primarily to the improved endosome escape endowed with CQ treatment. Therefore, D-R7H3 demonstrated a higher

enhancement in transfection efficiency than D-R5H5 with moderate buffering capacity. D-R3H7 with the highest buffering capacity probably realized the optimal endosome escape. CQ treatment could cause the untimely/too fast endosomal escape of D-R3H7/pDNA polyplexes, thereby affecting the intracellular transportation of pDNA into the cell nucleus and resulting in a lower transfection.

D-R7H3-, D-R5H5-, and D-R3H7/pDNA polyplexes at the N/P ratio of 10 demonstrated a significantly decreased luciferase expression after CQ treatment (Figure 10). This study further confirmed that such untimely/premature endosome escape would compromise the gene delivery efficiency or cause toxicity. Several evidences can support this conclusion. First, for the D-RxHy lacking buffering group (H), the higher amount of free D-RxHy in polyplexes at high N/P ratios would benefit endosomal escape [18,30]. For example, D-R7H3 (with the lowest buffering capacity) demonstrated an obviously enhanced transfection efficiency with increasing N/P ratio from 2 to 10 (Figure 5 and 6). Next, CQ further decreased the transfection efficiency of D-R3H7 that contains the highest buffering capacity with increasing N/P ratio from 2 to 10. All the results above suggested that both the timing and efficiency of endosome escape are equally important. Therefore, gene transfection requires the vector with well-balanced properties that can be finely tuned to match the extremely narrow window of transfection. To realize the full potential of the polymer-based nucleic acid delivery system, we may have to elucidate the molecular mechanism of the transfection. Through this study, we demonstrated that the D-RxHy platform could provide finely tuned properties over a large window. We believe it can be a powerful tool that allows us to study the molecular aspects of transfection in more detail.

#### **4. Conclusions**

In this study, five dextran-peptide vectors (D-RxHy) were prepared via grafting different cationic peptides to dextran backbones for gene delivery. We developed a further understanding on how the structure of the cationic peptide affected the transfection behaviors of D-RxHy vectors. Compared to other D-RxHy vectors, the D-R3H7 vector derived from H-rich peptide (R3H7C) possessed the highest DNA-binding ability among the five D-RxHy vectors, and achieved a similarly low cytotoxicity. The well-balanced H/R ratio in cationic peptides was crucial in the transfection performance of the corresponding D-RxHy vectors. D-R5H5 mediated a similarly high cell uptake rate with D-R3H7 at a low N/P ratio of 2, owing to the high H residues. D-R3H7 possessed the highest buffer capacity owing to the highest H content. Meanwhile, D-R3H7 exhibited the highest luciferase expression level among the five D-RxHy vectors even at the low N/P ratio of 2, indicating the efficient high-loading gene delivery. In this study, D-R3H7/pDNA polyplexes, endowed by the incorporation of a high amount of H residues, demonstrated the excellent potential for gene delivery at a low N/P ratio. The present work indicated that the D-R3H7 vector with rich H groups may be a promising delivery system for efficient high-loading gene therapy.

#### **Acknowledgements**

This work is supported by the US National Science Foundation (DMR-1454837, DMR-1206923) and National Natural Science Foundation of China (51528301, 51703008 and 51829301).

#### **Appendix A. Supplementary data**

Data of additional characterization such as  $^1\text{H}$  NMR spectra of polymers and EGFP expression of PEI/pEGFP-N1 polyplexes can be found in the supporting information.

## References

- [1] Morille M, Passirani C, Vonarbourg A, Clavreul A, Benoit JP. Progress in developing cationic vectors for non-viral systemic gene therapy against cancer. *Biomaterials* 2008; 29: 3477-96.
- [2] Johnson LA, Morgan RA, Dudley ME, Cassard L, Yang JC, et al. Gene therapy with human and mouse T-cell receptors mediates cancer regression and targets normal tissues expressing cognate antigen. *Blood* 2009; 114: 535-46.
- [3] Bainbridge JW, Smith AJ, Barker SS, Robbie S, Henderson R, et al. Effect of gene therapy on visual function in Leber's congenital amaurosis. *New Engl J Med* 2008; 358: 2231-9.
- [4] Ran FA, Hsu PD, Lin CY, Gootenberg JS, Konermann S, et al. (2013). Double nicking by RNA-guided CRISPR Cas9 for enhanced genome editing specificity. *Cell* 2013; 154: 1380-9.
- [5] Shalem O, Sanjana NE, Hartenian E, Shi X, Scott DA, et al. Genome-scale CRISPR-Cas9 knockout screening in human cells. *Science* 2014; 343: 84-7.
- [6] Mintzer MA, Simanek EE. Nonviral vectors for gene delivery. *Chem Rev* 2008; 109: 259-302.
- [7] Wang HY, Yi WJ, Qin SY, Li C, Zhuo RX, Zhang XZ. Tyrosine-leucine-based gene vector for suppressing VEGF expression in cancer therapy. *Biomaterials* 2012; 33: 8685-94.
- [8] Yin H, Kanasty RL, Eltoukhy AA, Vegas AJ, Dorkin JR, et al. Non-viral vectors for gene-based therapy. *Nat Rev Genet* 2014; 15: 541-55.
- [9] Khan W, Hosseinkhani H, Ickowicz D, Hong PD, Yu DS, Domb AJ. Polysaccharide gene transfection agents. *Acta Biomaterialia* 2012; 8: 4224-32.
- [10] Kwon OJ, Kang E, Choi JW, Kim SW, Yun CO. Therapeutic targeting of chitosan-PEG-folate-complexed oncolytic adenovirus for active and systemic cancer gene therapy. *J Control Release* 2013; 169: 257-65.
- [11] Zhao X, Li Z, Pan H, Liu W, Lv M, et al. Enhanced gene delivery by chitosan-disulfide-conjugated LMW-PEI for facilitating osteogenic differentiation. *Acta Biomater* 2013; 9: 6694-703.
- [12] Lu H, Wang J, Song Z, Yin L, Zhang Y, et al. Recent advances in amino acid N-carboxyanhydrides and synthetic polypeptides: chemistry, self-assembly and biological applications. *Chem Commun* 2014; 50: 139-55.
- [13] Yao H, Wang K, Wang Y, Wang S, Li J, et al. Enhanced blood-brain barrier penetration and glioma therapy mediated by a new peptide modified gene delivery system. *Biomaterials* 2015; 37: 345-52.
- [14] Tang Q, Cao B, Wu H, Cheng G. Selective gene delivery to cancer cells using an integrated cationic amphiphilic peptide. *Langmuir* 2012; 28: 16126-32.
- [15] Yang J, Liu Y, Wang H, Liu L, Wang W, et al. The biocompatibility of fatty acid modified dextran-arginine bioconjugate gene delivery vector. *Biomaterials* 2012; 33: 604-13.

- [16] Hu Y, Zhu Y, Yang WT, Xu FJ. New star-shaped carriers composed of  $\beta$ -cyclodextrin cores and disulfide-linked poly (glycidyl methacrylate) derivative arms with plentiful flanking secondary amine and hydroxyl groups for highly efficient gene delivery. *ACS Appl Mater Interfaces* 2013; 5: 703-12.
- [17] Yang, XC, Niu YL, Zhao NN, Mao C, Xu FJ. A biocleavable pullulan-based vector via ATRP for liver cell-targeting gene delivery. *Biomaterials* 2014; 35: 3873-84.
- [18] Thibault M, Astolfi M, Tran-Khanh N, Lavertu M, Darras V, et al. Excess polycation mediates efficient chitosan-based gene transfer by promoting lysosomal release of the polyplexes. *Biomaterials* 2011; 32: 4639-46.
- [19] Chang KL, Higuchi Y, Kawakami S, Yamashita F, Hashida M. Efficient gene transfection by histidine-modified chitosan through enhancement of endosomal escape. *Bioconjug Chem* 2010; 21: 1087-95.
- [20] Kos P, Lächelt U, Herrmann A, Mickler FM, Döblinger M, et al. Histidine-rich stabilized polyplexes for cMet-directed tumor-targeted gene transfer. *Nanoscale* 2015; 7: 5350-62.
- [21] Meng Z, Luan L, Kang Z, Feng, S, Meng Q, et al. Histidine-enriched multifunctional peptide vectors with enhanced cellular uptake and endosomal escape for gene delivery. *J Mater Chem B* 2017; 5: 74-84.
- [22] Tang Q, Cao B, Lei X, Sun B, Zhang Y, et al. Dextran-peptide hybrid for efficient gene delivery. *Langmuir* 2014; 30: 5202-8.
- [23] vanDijkWolthuis WNE, KettenesvandenBosch JJ, vanderKerkvanHoof A, Hennink WE. Reaction of dextran with glycidyl methacrylate: An unexpected transesterification. *Macromolecules* 1997; 30: 3411-3.
- [24] Hu Y, Zhao N, Yu B, Liu F, Xu FJ. Versatile types of polysaccharide-based supramolecular polycation/pDNA nanoplexes for gene delivery. *Nanoscale* 2014; 6: 7560-9.
- [25] Mumper RJ, Duguid JG, Anwer K, Barron MK, Nitta H, et al. (1996). Polyvinyl derivatives as novel interactive polymers for controlled gene delivery to muscle. *Pharm Res* 1996, 13: 701-9.
- [26] Wang ZH, Zhu Y, Chai MY, Yang WT, Xu FJ. Biocleavable comb-shaped gene carriers from dextran backbones with bioreducible ATRP initiation sites. *Biomaterials* 2012; 33: 1873-1883.
- [27] Erbacher P, Roche AC, Monsigny M, Midoux P. Putative role of chloroquine in gene transfer into a human hepatoma cell line by DNA lactosylated polylysine complexes. *Exp Cell Res* 1996; 225: 186-94.
- [28] Bhattarai SR, Muthuswamy E, Wani A, Brichacek M, Castañeda AL, et al. Enhanced gene and siRNA delivery by polycation-modified mesoporous silica nanoparticles loaded with chloroquine. *Pharm Res* 2010; 27: 2556-68.

- [29] Li M, Schlesiger S, Knauer SK, Schmuck C. A tailor-made specific anion-binding motif in the side chain transforms a tetrapeptide into an efficient vector for gene delivery. *Angew Chem Int Ed* 2015; 54: 2941-4.
- [30] Huang M, Fong CW, Khor E, Lim LY. Transfection efficiency of chitosan vectors: effect of polymer molecular weight and degree of deacetylation. *J Control Release* 2005; 106: 391-406.

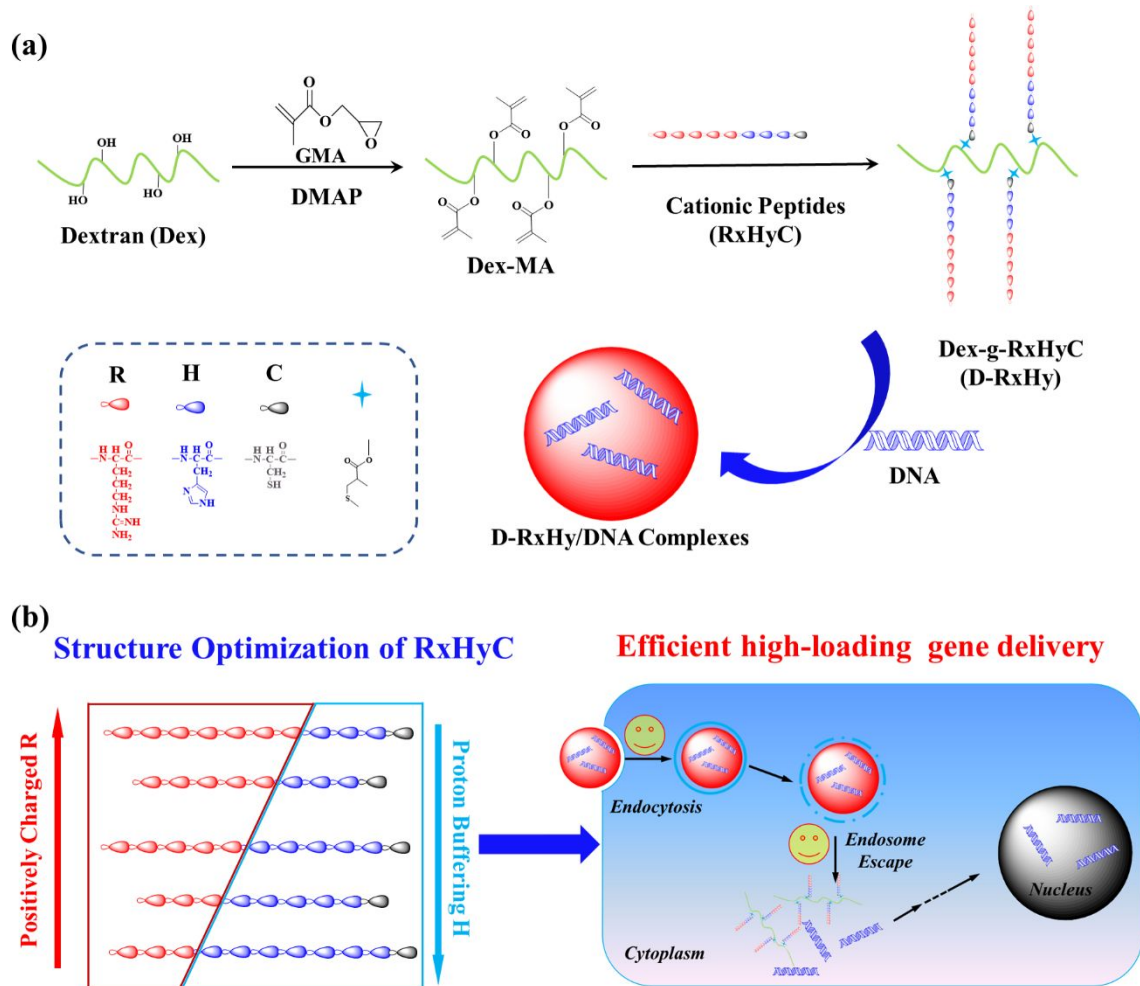


**Fig. 1.** Schematic diagram illustrating (a) the preparation processes of D-RxHy vectors and (b) the optimization of efficient high-loading gene delivery.

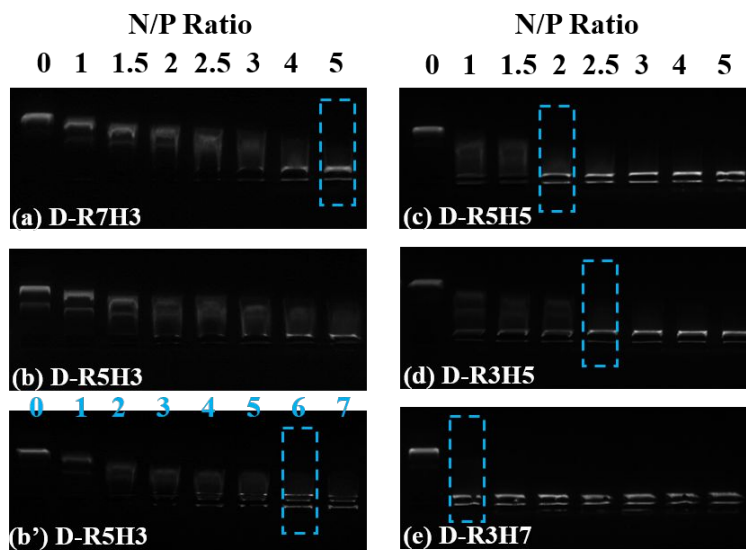


**Fig. 2.** Electrophoretic mobility of pDNA in the polyplexes of the cationic polymers ((a) D-R7H3, (b, b') D-R5H3, (c) D-R5H5, (d) D-R3H5, and (e) D-R3H7 at various N/P ratios (The blue box indicates the threshold N/P ratio of condensing pDNA into positively charged polyplexes).

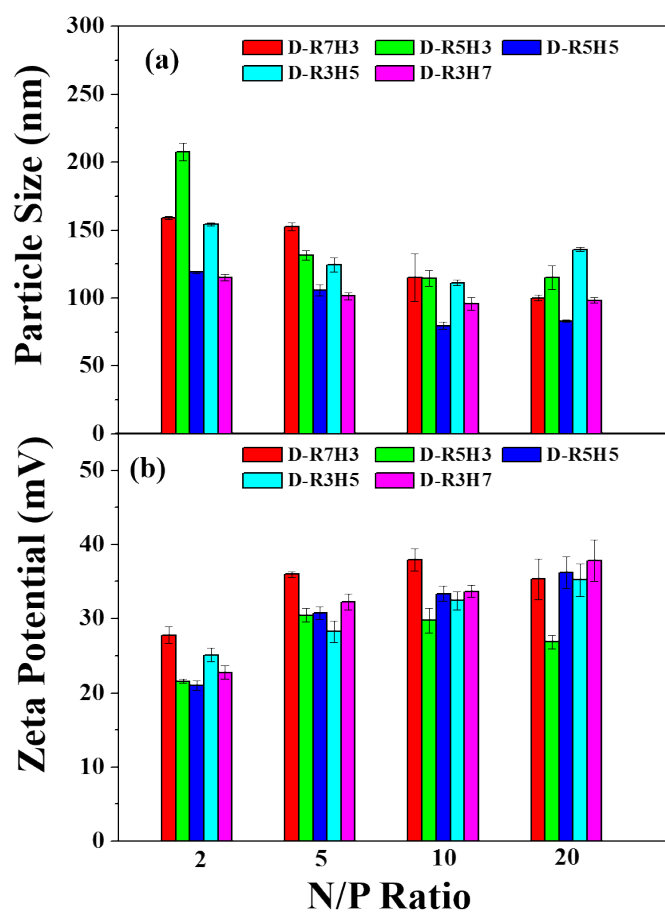


**Fig. 3.** (a) Particle size and (b) zeta potential of the D-RxHy/pDNA polyplexes in water at various N/P ratios. (mean  $\pm$  SD, n = 3).

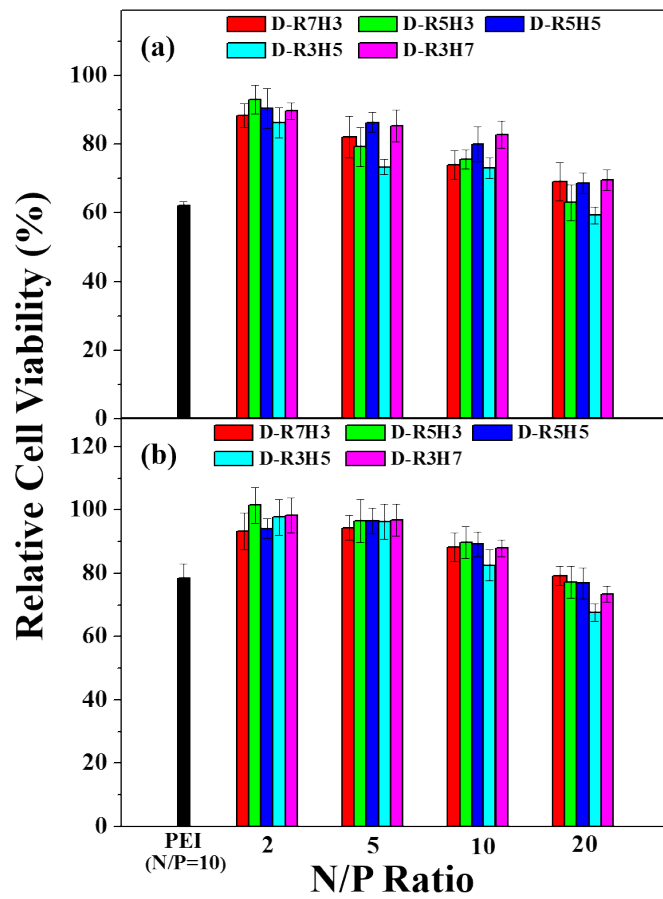


**Fig. 4.** Cell viability of D-RxHy/pDNA polyplexes at different N/P ratios in comparison with PEI/DNA polyplex (at its optimal N/P ratio of 10) in (a) COS 7 and (b) MCF7 cell lines (mean  $\pm$  SD, n = 6).

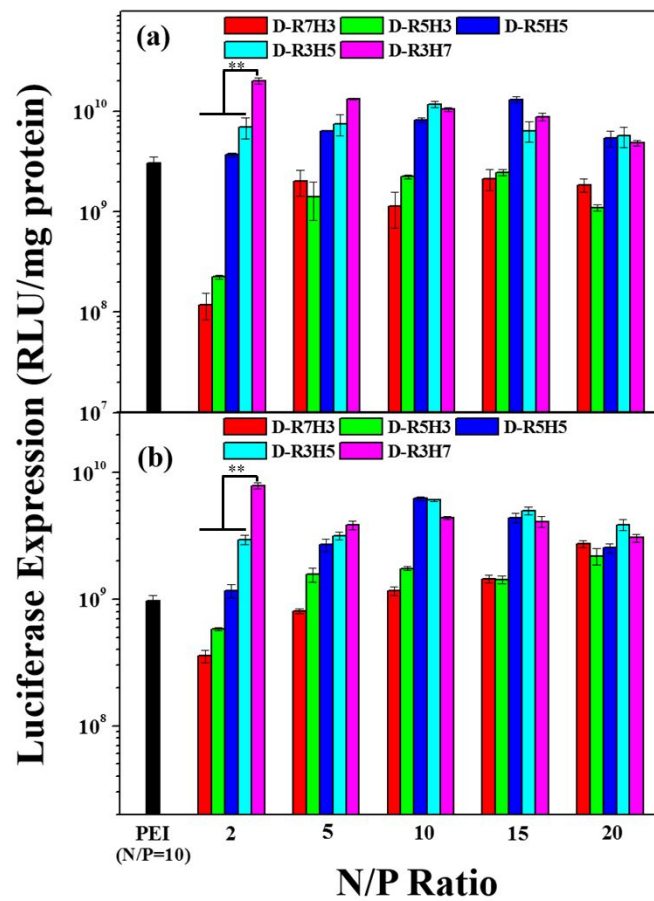


**Fig. 5.** In vitro gene transfection efficiency of D-RxHy/pDNA polyplexes at different N/P ratios in comparison with PEI/pDNA polyplex (at its optimal N/P ratio of 10) in (a) COS7 and (b) MCF7 cell lines (mean  $\pm$  SD,  $n = 3$ , \*\* $P < 0.01$ ).

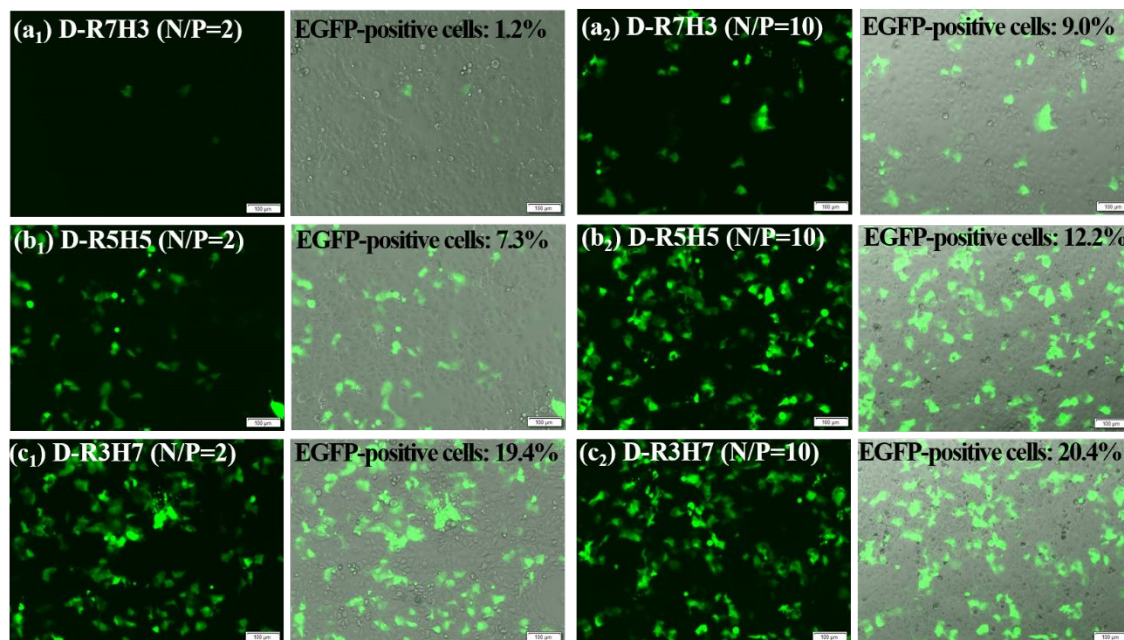


**Fig. 6.** In vitro EGFP expression of pEGFP-N1 polyplexes of (a<sub>1</sub> and a<sub>2</sub>) D-R7H3, (b<sub>1</sub> and b<sub>2</sub>) D-R5H5 and (c<sub>1</sub> and c<sub>2</sub>) D-R3H7 in MCF7 cells (a<sub>1</sub>,b<sub>1</sub>,c<sub>1</sub>: polyplexes at the N/P ratio of 2; a<sub>2</sub>,b<sub>2</sub>,c<sub>2</sub>: polyplexes at the N/P ratio of 10), where the percentages of EGFP-positive cells were determined by flow cytometry.

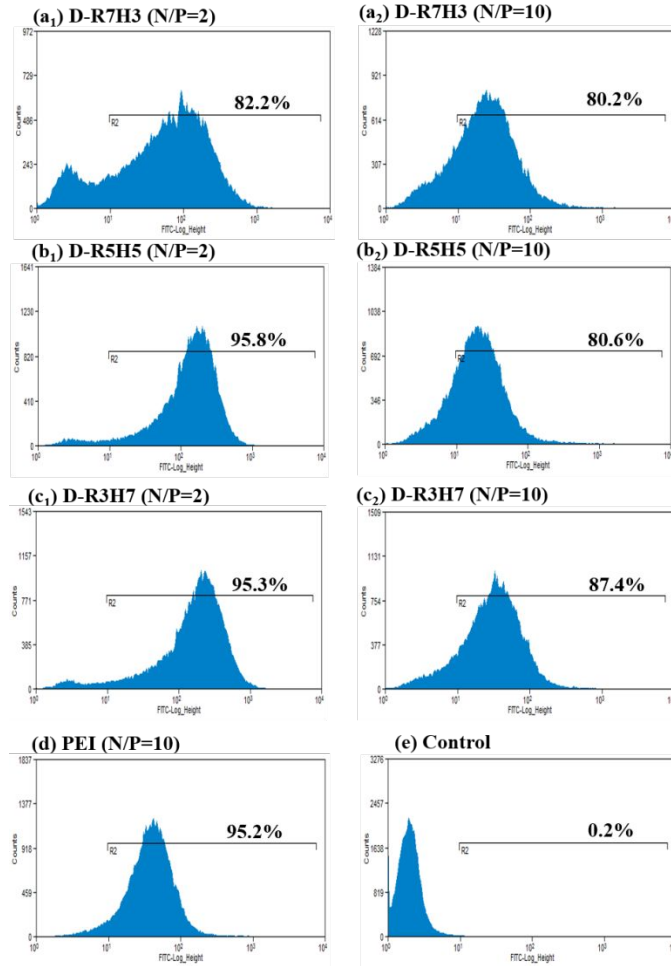


**Fig. 7.** Cellular internalization of YOYO-labelled pDNA in the polyplexes of (a<sub>1</sub> and a<sub>2</sub>) D-R7H3, (b<sub>1</sub> and b<sub>2</sub>) D-R5H5 and (c<sub>1</sub> and c<sub>2</sub>) D-R3H7 in MCF7 cells (a<sub>1</sub>,b<sub>1</sub>,c<sub>1</sub>: polyplexes at the N/P ratio of 2; a<sub>2</sub>,b<sub>2</sub>,c<sub>2</sub>: polyplexes at the N/P ratio of 10), in comparison with that of (d)PEI/pDNA at the N/P ratio of 10 and (e) blank control.

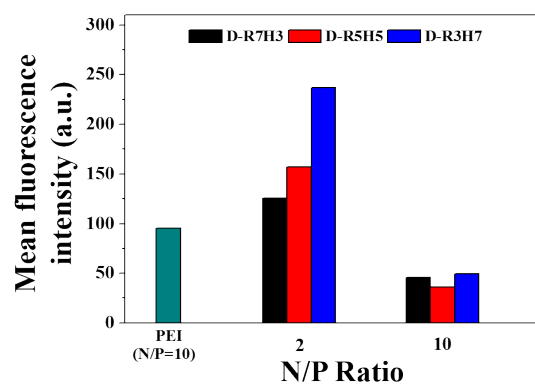


**Fig. 8.** Quantitative analysis of green fluorescence intensity of MCF7 cells after incubation 4 hours with YOYO-labelled pDNA in the polyplexes of D-R7H3, D-R5H5, D-R3H7, and PEI using flow cytometry.

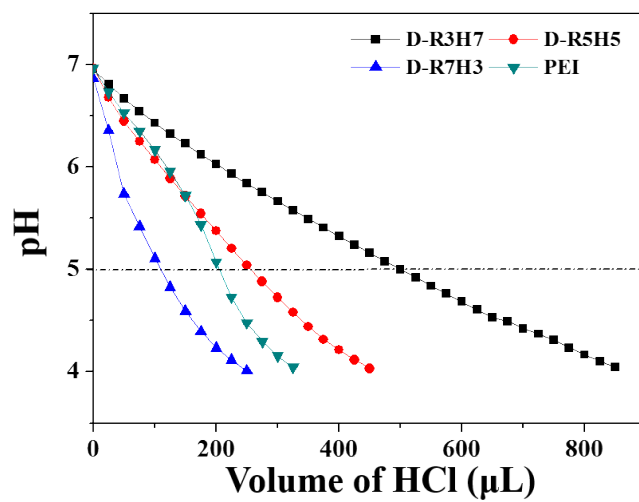


**Fig. 9.** Determination of the buffer capacity of D-R7H3, D-R5H5, D-R3H7, and PEI by acid–base titration, where the cationic polymer solutions with 1 mM cationic group (R residue for D-RxHy and amino group for PEI) concentration were titrated with 0.01 N HCl solution.

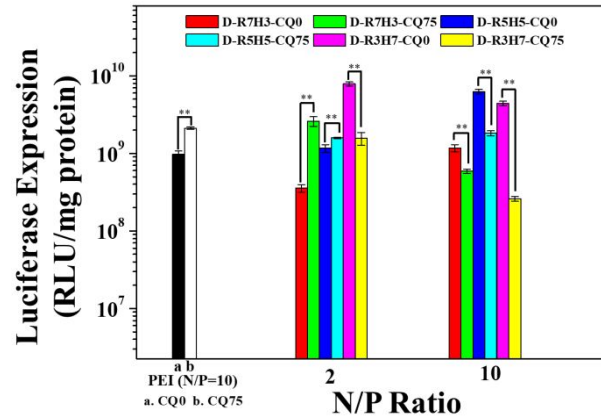


**Fig. 10.** In vitro gene transfection efficiency of the D-RxHy/pDNA polyplexes (a) at various N/P ratios in the absence and presence of 75  $\mu$ M concentration of CQ, in comparison with that mediated by PEI (at its optimal N/P ratio of 10) in MCF7 cells (mean  $\pm$  SD, n = 3, \*\*P<0.01).